CMS Physics Analysis Summary

Contact: cms-pog-conveners-btag@cern.ch 2009/08/08

Impact of Tracker Misalignment on the CMS b-Tagging Performance

The CMS Collaboration

Abstract

The expected performance of b-tagging algorithms is studied for various scenarios in which realistic detector effects corresponding to the first data taking phase of the experiment are taken into account, for example silicon tracker misalignment corresponding to first collisions, as well as to 10 and 100 pb^{-1} of integrated luminosity. A simple secondary vertex algorithm is investigated, based purely on the presence of a reconstructed secondary vertex, that is robust with respect to misalignment and has a light flavor mistagging rate of below 3% for a b-tagging efficiency of 35% for the expected startup tracker misalignment conditions.

1 Introduction

The identification of jets originating from the hadronization of b-quarks is a crucial tool for a large number of physics analyses in CMS, such as top quark physics, the search for the Higgs boson or for new physics beyond the standard model. Several methods exist to distinguish b-jets from non-b-jets. Most of these methods rely on the fact that a b-hadron has a significant lifetime of $\tau \approx 1.5$ ps (with $c\tau \approx 450$ μm). This lifetime leads to a displacement of the b-hadron's decay vertex from the primary vertex of the event. Tracks emerging from this decay vertex provide an "impact parameter" which is defined as the minimum distance of the linearized track from the primary vertex. Furthermore, a secondary vertex can be reconstructed from tracks belonging to the b-hadron decay.

The performance of the b-tagging algorithms is directly coupled to the performance of the track and vertex reconstruction, which in turn directly depends on the alignment of the CMS silicon tracker, i.e. the precise knowledge of the exact positions and orientations of its around 16,000 detector modules. At the beginning of data taking, tracker misalignment (e.g. due to limited mounting precision of sensors, moving structures due to thermal and magnetic field effects etc.) will considerably impact the hit position errors and the reconstruction of tracks and vertices as well as the associated measurement errors.

In this paper, the impact (in terms of robustness) of various degrees of tracker misalignment on the different b-tagging algorithms used in CMS is studied for several "misalignment scenarios" [1], which are supposed to mimic detector configurations to be expected during the early phases of data taking:

- **Startup Scenario:** The tracker alignment precision in this scenario is supposed to resemble the conditions at the first collisions in CMS. In this case, only information from survey measurements, the Laser Alignment System and cosmic muon tracks can be used to perform a detector alignment.
- **10 pb^{-1} Scenario:** In this scenario, it is assumed that the tracker can be aligned by using cosmic muon data and a sample of collision tracks, mainly being isolated hadrons in minimum bias events and muons from the decays of low mass resonances like J/ψ and Upsilon. For the pixel detector, it is assumed that the alignment of its larger structures can be improved by a factor of 5, but that there is no improvement of the module-level alignment. For the strip tracker, it is assumed that the sub-detector positions can be aligned with an accuracy of 100 μm .
- **100 pb^{-1} Scenario:** For 100 pb^{-1} of collected data, high p_T muons from Z and W boson decays are available in significant quantity, in addition to the previously mentioned data. The misalignment of the pixel tracker is expected to be $\mathcal{O}(20\ \mu\text{m})$, and that of the strip tracker $\mathcal{O}(30 \ldots 50\ \mu\text{m})$.
- **10 pb^{-1} Pixel L1 OFF Scenario:** A deactivation of certain parts of the pixel detector might occur for safety reasons especially during the early phase of operation. For the studies presented in the following sections, we use a scenario with misalignments as for the 10 pb^{-1} scenario, but where the innermost layer of the pixel detector is disabled.

Tracker misalignment is introduced at the reconstruction level. This means that hits are still reconstructed assuming a perfectly aligned detector. Afterwards, the detector components are randomly shifted and rotated by an appropriate amount defined by the misalignment scenario. In order to account for the introduced uncertainty on the hit position while searching for tracks an alignment position error (APE) is added in quadrature to the tracking hit error. The APE

recovers the track reconstruction efficiency from the otherwise reduced compatibility of the hits with the track candidates during pattern recognition. The APE is set corresponding to the overall misalignment of a silicon module. In real data, as the misalignment is not known, a choice must be made for the APE to be applied. In this respect, the scenarios are somewhat idealized. The full track reconstruction, including pattern recognition and fitting is performed after applying the misalignment.

The studies presented in the following sections have been performed using a sample of 20K inclusive $t\bar{t}$ events produced with PYTHIA 6, which have been reprocessed for the various detector configurations considered.

Jets are reconstructed from calorimeter towers using the iterative cone algorithm [2] with a cone size of 0.5. For the identification of the true flavour of the jets, a definition is used where the assumed jet flavour is the flavour that most probably determines the behaviour of the jet [1]. In all distributions shown, jets are selected with transverse momentum and pseudo-rapidity in the range $30 < p_T < 120$ GeV and $|\eta| < 2.4$, respectively.

Tracks are reconstructed using the standard Combinatorial Kalman Filter algorithm [3]. The track selection cuts, as well as the algorithms and selections applied during the reconstruction of primary and secondary vertices, correspond to the CMS default configuration, as documented in [2, 4–6] and references therein.

2 Behaviour of Observables

The most basic b-tagging algorithms rely exclusively on the impact parameters (I.P.) of tracks within a jet. In particular, the significance of the signed impact parameter defined as $sign \cdot \frac{value_{IP}}{error_{IP}}$ is used as discriminating variable in the taggers. The $sign$ is positive (negative) if the b-hadron decay occurs downstream (upstream) with respect to the jet direction [7].

Figure 1 shows the distribution of the transverse impact parameter significance for the misalignment scenarios and for different jet flavors. In these figures, the second track, ordered by the value of the I.P. significance is used because the first track has a high probability to be mismeasured. It is visible that the I.P. significance decreases for all flavors with increasing misalignment. The b-jets are affected the most. With larger misalignment, the distribution for b-jets gets more similar to the distribution of light flavor jets.

This behaviour is due to the increasing *error* of the impact parameter measurement which is illustrated in Figure 2. This Figure shows the distribution of the $error_{IP}$, while Figure 3 shows the distribution of the $value_{IP}$. In case of b-jets , the $value$ of the impact parameter is not affected very much since it is big because of the lifetime, but the corresponding *error* increases. For light flavour jets, the significance decreases, because the tails of the distribution are caused by badly reconstructed tracks, not described by a gaussian σ. However, in the core of the distribution for light flavours, the significance should remain unchanged.

The observed excess at positive values of the impact parameter significance distribution for light flavour jets in case of the startup misalignment scenario (Figure 1) is due to the large rate of fake or mismeasured tracks in these conditions.

The secondary vertex reconstruction algorithm uses an adaptive vertex finding method [6]. Table 1 gives an overview of the secondary vertex reconstruction efficiencies obtained by the default configuration. The numbers reflect the fraction of jets where a secondary vertex is re-

[1] This means that if gluon splitting into $b\bar{b}$ occurs, the jet will be labeled as b-jet and not as gluon jet.

Table 1: Fraction (in %) of jets with a reconstructed secondary vertex for light flavour (udsg), charm and bottom jets, presented for various misalignment scenarios.

	Secondary vertex fraction [%]		
Misalignment scenario	b-jets	c-jets	udsg-jets
No Misalignment	62.6	22.0	2.7
100 pb^{-1} Misalignment	62.1	19.6	2.4
10 pb^{-1} Misalignment	53.0	12.7	2.9
10 pb^{-1} Pixel L1 Off Misal.	39.2	7.6	1.9
Startup Misalignment	37.8	7.7	3.5

constructed. While the vertex finding efficiency remains similar to the perfect alignment case for the 100 pb^{-1} scenario, a degradation is observed for larger misalignments. In general, the vertex finding efficiency drops in case of misalignment because tracks originating from secondary vertices which are located close to the primary vertex are associated with the primary vertex because of the increased track parameter errors. Vertices are also rejected by the secondary vertex finder because they fail the cuts on decay length significance and/or track impact parameter significance.

The "flight distance significance" is shown in Figure 4. It is defined as the measured separation (in 3D) of the reconstructed secondary vertex from the primary vertex, divided by the measurement error. In case of light flavour and gluon jets no real secondary vertices exist (except some negligible amount from V0 decays). Therefore all reconstructed vertices are regarded as fake vertices and the distribution of the flight distance significance for these jets is strongly peaked at small values. For c-quark and especially b-quark jets, there is a significant contribution of real displaced vertices, such that the flight distance significance distribution shows a large tail towards positive values. For large values of the flight distance itself, the distributions are fairly independent of the misalignment: if the secondary vertex is far enough displaced from the primary vertex, it will still be reconstructed. On the other hand, the increased measurement errors lead to a reduced flight distance significance.

Some further observables at the secondary vertex are shown (only for b-jets) in Figure 5, namely the track multiplicity, the energy fraction and the mass of the secondary vertex. They are found to be only weakly affected by misalignment.

3 Performance of the Algorithms

In this section the performances of the standard b-tagging algorithms in a misaligned detector are summarized. The performance is typically displayed as the misidentification rate versus b-tagging efficiency.

- The "track counting" algorithm [7] simply uses the impact parameter significance of a particular track as discriminator. The "high efficiency" algorithm uses the second track, while the "high purity" algorithm uses the third track, where the tracks are ordered by the impact parameter significance itself. The performance of these two algorithms is shown in Figures 6 and 7.
- The "jet probability" algorithm [7] also relies on the impact parameter significance, but in a more advanced way. It does not use a single track, but calculates the probability for a set of tracks to come from the primary vertex using a likelihood method

and separating the tracks into several categories. This algorithm has a better performance than the counting methods, but suffers from misalignment in a similar way, as visible in Figure 8. The algorithm uses likelihood probability density functions (PDFs) for various track categories, defined among others by means of the number of pixel hits. These PDFs have not been remade, which leads to a bias for the case in which the first pixel layer is switched off, since the maximum number of pixel hits is two instead of three. Due to this reason, the corresponding scenario has been left out in all "jet probability" plots presented here.

- Currently the most advanced algorithm is the "Combined Secondary Vertex" algorithm, which uses also information from secondary vertex properties, like the flight distance, and combines this with impact parameter information, using a likelihood discriminant. A detailed description of this algorithm is available in [8, 9], and its performance is presented in Figure 9.
- The soft lepton tagging algorithms exploit the presence of leptons in b-hadron decay chains. A leptonic decay occurs in 20% of the cases per lepton flavour (including cascade decays of the c-hadron). The kinematical properties of the lepton are used to calculate a discriminator [10]. Figures 10 and 11 show the performance of the two soft lepton tagging algorithms. As expected, the performance of these algorithms is much less affected by tracker misalignment even though they also include information about the impact parameters. However, their overall b-jet efficiency is only 5-10%.

It is interesting to note that even for the tracker misalignments expected at the beginning of data taking, lifetime based b-tagging algorithms can still be used to discriminate b-jets from light quark and gluon jets. Typically, in order to achieve a light flavor mistagging rate which is similar to the ideal detector case, the b-jet efficiency is reduced by 10-30%, depending on the degree of misalignment. The reduction is stronger in case of the startup scenario.

For a better comparison of the behaviour of the different algorithms, the relative decrease in performance is shown in Figure 12 for the light flavor mistagging rate and in Figure 13 for the charm mistagging rate. Here, the relative performance decrease is simply defined as the ratio of efficiencies $\epsilon^{mistag}_{misalign}/\epsilon^{mistag}_{align}$ for a given b-tagging efficiency. Since charm-jets have a similar topology as b-jets, the charm tagging efficiency is correlated to the b-tagging efficiency. This explains the observation that the relative performance decrease is smaller for charm mistags than for light flavor mistags.

The distributions show that the various algorithms react quite differently to the misalignment scenarios. While the soft lepton algorithms do not depend a lot on the degree of tracker misalignment, algorithms based on track impact parameters and/or secondary vertices are strongly affected, as expected. The performance of the Combined Secondary Vertex algorithm is affected the most. This is to be expected as it combines impact parameter as well as secondary vertex information in a sensitive way and requires careful training of the PDFs used in the likelihood discriminant.

The focus of this note is to present the actual impact of various degrees of misalignment on the performance of the b-tagging algorithms. In practice, the b-jet efficiencies as well as the light jet mistagging rates have to be measured from the data themselves. Various methods to achieve this have already been studied in [11, 12]. The results will be compared with the performance extracted from simulation. Differences may arise for example due to imperfect detector simulation, deviations of the actual from the true track reconstruction performance, or the fact that the alignment constants used in the simulation do not match the actual ones.

In physics analyses using simulated Monte Carlo samples then either the tabulated measured performances can be used, or the simulated performances can be calibrated to the measured values.

A further complication arises in the case of b-tagging algorithms which rely on the training of likelihood PDFs or other multivariate discriminants using information about the true jet flavour in simulated events, for example the jet probability and combined secondary vertex algorithms. This training requires large event samples and will be done using events simulated with the by then best knowledge of the tracker geometry. In particular at the beginning of data taking, a significant uncertainty will be associated with the determined tracker alignment, and hence the training will not be ideal, in addition to the already degraded tracking performance. In view of these aspects it is considered unlikely that algorithms such as jet probability or Combined Secondary Vertex will be useable in the early data taking phase.

4 Study of a Simple Secondary Vertex Algorithm

In this section a b-tagging algorithm is studied which is suitable for the early data taking period. It should be robust, meaning that its performance should not strongly depend on the degree of misalignment. It should also be simple, such that its performance is comparatively easy to determine. In particular, it should not rely on the training of a likelihood or other multivariate discriminant.

The robustness of the observables at the secondary vertex suggests to use a b-tagging algorithm which only relies on this kind of observables. For the algorithm to be useable in startup conditions, it should avoid complex methods of combining several observables with e.g. likelihood or even more sophisticated approaches. Therefore, the resulting algorithm only relies upon the presence of a secondary vertex. The maximum b-tagging efficiency is of course limited by the reconstruction efficiency of a secondary vertex within the assumed b-jet. Such simple secondary vertex algorithms are also often used at other experiments.

In addition to requiring the successful reconstruction of a secondary vertex, one variable derived from that vertex can be directly used as discriminator upon which can be cut to choose an appropriate working point. As discriminator candidates four promising secondary vertex observables have been chosen and tested on their robustness against misalignment, namely the four combinations of value and significance of the flight distance between primary and secondary vertex in both two and three dimensions. As all share a similar robustness and the flight distance significance taggers perform comparably or even better than the taggers relying on the flight distance value, the tagger based on the 3D flight distance significance is chosen.

Figure 14 shows the b-tagging performance of the simple secondary vertex tagger in comparison to several other b-tagging algorithms presented earlier in this note. It can be seen that even this simple tagger has quite some discrimination power and allows a sufficiently good background reduction for light flavor and charm jets. Figure 15 shows the relative performance decrease for the simple secondary vertex tagger compared to a perfectly aligned tracker along with other b-tagging algorithms. For light flavor jets, the performance decrease is less than a factor of 2 over the whole b-tagging efficiency range whereas for most other taggers a decrease in performance up to a factor of 10 or even more occurs. The explanation for the robustness of the simple secondary vertex tagger is the fact that the flight distance significance behaves in a similar way for the different flavours if misalignment is applied.

A remarkable feature arises in the case of the charm mistagging rate, where the rejection perfor-

mance improves with increasing misalignment. This behaviour can be explained by the choice of the default cuts in the secondary vertex reconstruction. A charm decay is very similar to a b-hadron decay. It also has a real displaced secondary vertex, but with a smaller separation from the primary vertex as well as a smaller track multiplicity. This small separation is more difficult to measure than the larger separation of the b-hadron, especially if the measurement precision degrades. Therefore a decreased measurement precision has a larger impact on the charm vertex reconstruction efficiency than on the b efficiency. The result is that in case of misalignment, more secondary vertices originating from charm hadron decays cannot be separated from the primary vertex leading to a decrease of the charm mistagging rate.

A detailed systematic study has been carried out in which the default configuration parameters of the track selection and the secondary vertex reconstruction were varied. No further improvement with respect to the robustness of the algorithm could be found.

5 Alignment Position Error Variations

The optimal choice for the alignment position error (APE) used during track reconstruction with tracking system misalignment has been assumed for this study. However, with real data, the APE can only be estimated and therefore a variation by a factor of 2 for the value has been studied for the 10 pb^{-1} misalignment scenario to estimate the potential additional effects on the performance.

Figure 16 shows the results for the "high efficiency track counting" and simple secondary vertex algorithm. The effects of choosing a too large APE are comparable to the observations made when the measure of misalignment increases, i.e. the higher track fake rate and more badly measured tracks cause an increase in the mistagging rate for the impact parameter based algorithms in the high purity region. For the secondary vertex based algorithm, there is a small increase in mistagging rate and more notably a significant decrease in secondary vertex finding efficiency. For a too small choice of the APE, there is a slight performance improvement visible due to a stronger fake track suppression effect. This can be interpreted as an indication that there is room for optimization of the b-tagging track selection cuts for the misalignment scenarios, which however, would have to be conducted using real data measurements since the errors are effectively unknown. For even smaller APEs this effect gets dominated by a decline in b-jet tagging efficiency due to decreased tracking efficiency.

6 Conclusions

The performances of all standard CMS b-tagging algorithms for the tracker misalignment scenarios have been presented and the relative performance decrease has been compared. The various algorithms react to misalignments in different ways. In general algorithms relying on track impact parameters and/or secondary vertex properties are much more sensitive to misalignments than soft lepton algorithms. However, the latter suffer from a low overall b-tagging efficiencies.

Nevertheless, even for the tracker misalignments expected at the beginning of data taking, lifetime based b-tagging algorithms can be used to discriminate b-jets from light quark and gluon jets. For a light flavor mistagging rate similar to the ideal detector case, the b-jet efficiency is reduced by 10-30%, depending on the degree of misalignment.

A simple secondary vertex tagger has been studied which is robust and has a sufficient performance at the same time. This algorithm only uses the flight distance significance of the

secondary vertex as discriminator. It has been shown that for both the 10 pb^{-1} and startup scenarios, this tagger provides a light flavor mistagging rate of below 3% for a b-tagging efficiency of 35%.

References

[1] T. Lampen, N. de Filippis, F.-P. Schilling, A. Schmidt, and M. Weber, "Comprehensive Set of Misalignment Scenarios for the CMS Tracker," *CMS Note* **2008/xyz** (2008). in preparation.

[2] CMS Collaboration, "The CMS Physics Technical Design Report, Volume 1: Detector Performace and Software," *CERN/LHCC* **2006-001** (2006). CMS TDR 8.1.

[3] W. Adam, B. Mangano, T. Speer, and T. Todorov, "Track reconstruction in the CMS tracker," *CMS Note* **2006/041** (2006).

[4] P. Vanlaer, V. Barbone, N. De Filippis, T. Speer, O. Buchmueller, and F.-P. Schilling, "Impact of CMS Silicon Tracker Misalignment on Track and Vertex Reconstruction," *CMS Note* **2006/029** (2006).

[5] T. Muller, C. Piasecki, G. Quast, and C. Weiser, "Inclusive Secondary Vertex Reconstruction in Jets," *CMS Note* **2006/027** (2006).

[6] T. Speer et al., "Vertex Fitting in the CMS Tracker," *CMS Note* **2006/032** (2006).

[7] A. Rizzi, F. Palla, and G. Segneri, "Track impact parameter based b-tagging with CMS," *CMS Note* **2006/019** (2006).

[8] C. Weiser, "A Combined Secondary Vertex Based B-Tagging Algorithm in CMS," *CMS Note* **2006/014** (2006).

[9] CMS Collaboration, "The CMS Physics Technical Design Report, Volume 2: Physics Performance," *CERN/LHCC* **2006-021** (2006). CMS TDR 8.2.

[10] A. Bocci, P. Demin, R. Ranieri, and S. de Visscher, "Tagging b jets with electrons and muons at CMS," *CMS Note* **2006/043** (2006).

[11] CMS Collaboration, "Performance Measurement of b-tagging Algorithms Using Data containing Muons within Jets," *CMS PAS* **BTV_07_001** (2008).

[12] CMS Collaboration, "Evaluation of udsg Mistags for b-tagging using Negative Tags," *CMS PAS* **BTV_07_002** (2008).

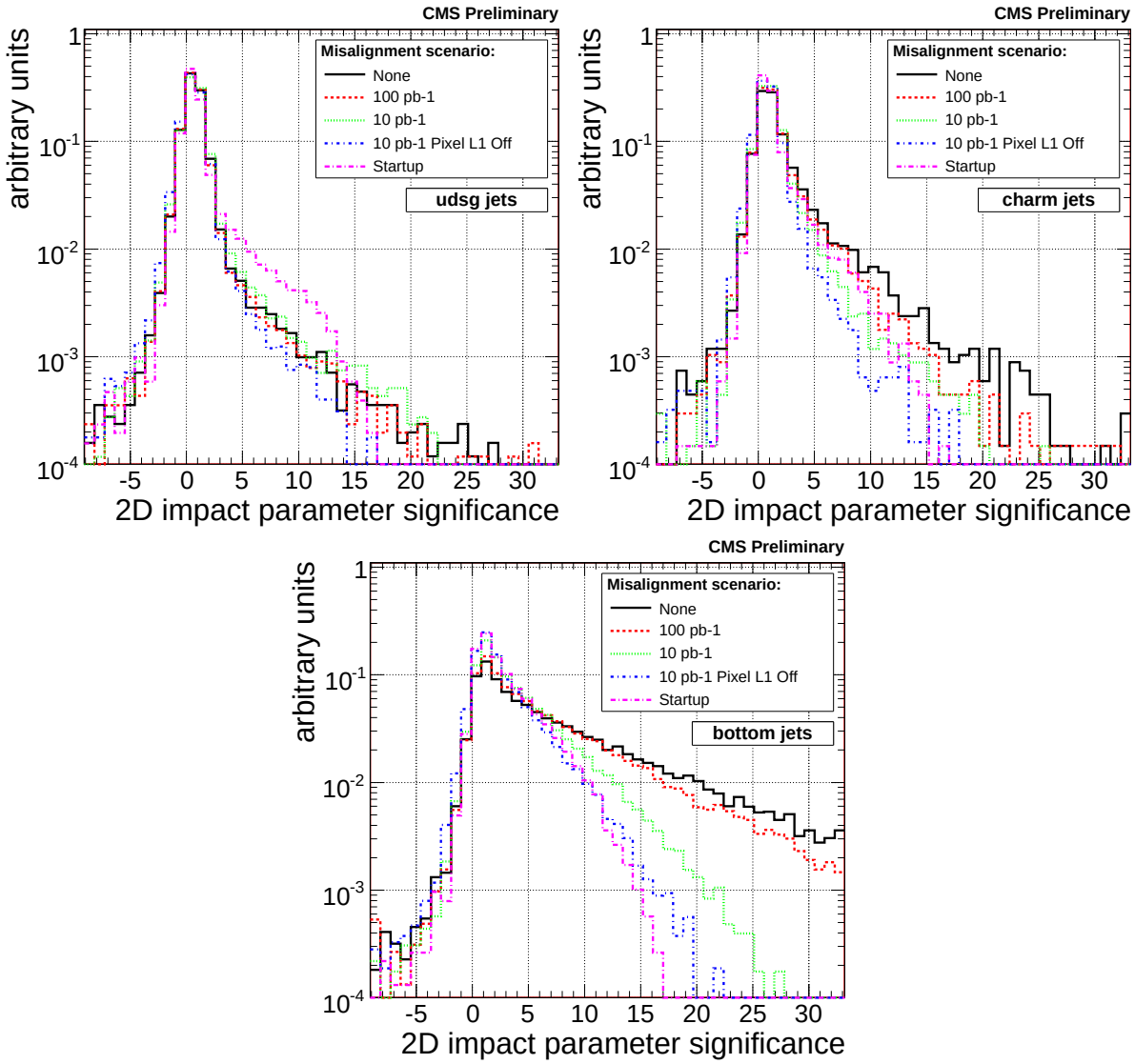

Figure 1: Distribution of the transverse impact parameter significance of the second track (ordered by I.P. significance) for the various scenarios and jet flavors, presented for light flavour jets (top left), charm jets (top right) and b-jets (bottom). Here and in the following figures, the term "light flavour jets" corresponds to jets originating from u, d and s quarks as well as from gluons.

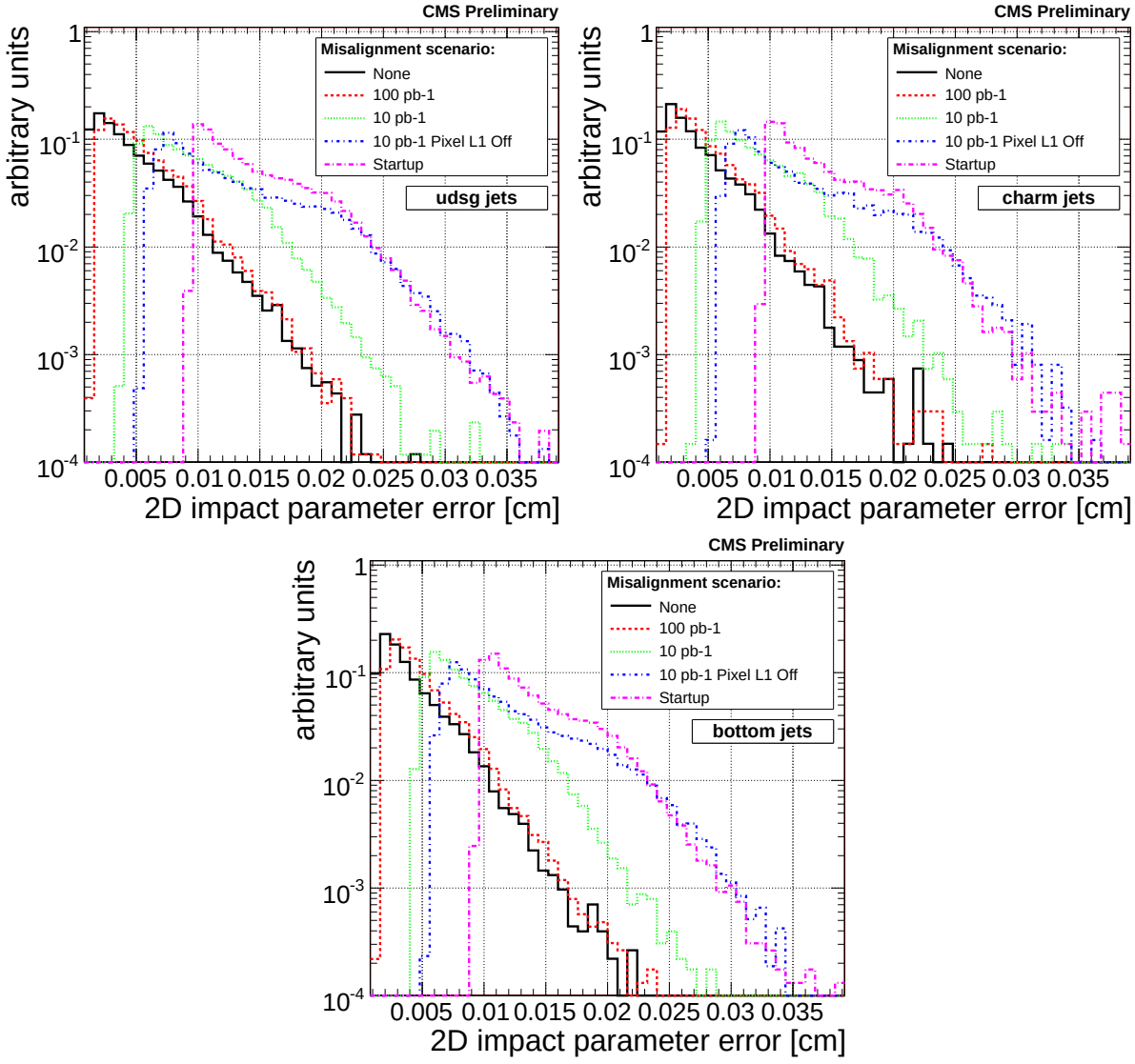

Figure 2: Distribution of the transverse impact parameter measurement *error* of the second track (ordered by I.P. significance) for the various scenarios and jet flavors, presented for light flavor jets (top left), charm jets (top right) and b-jets (bottom).

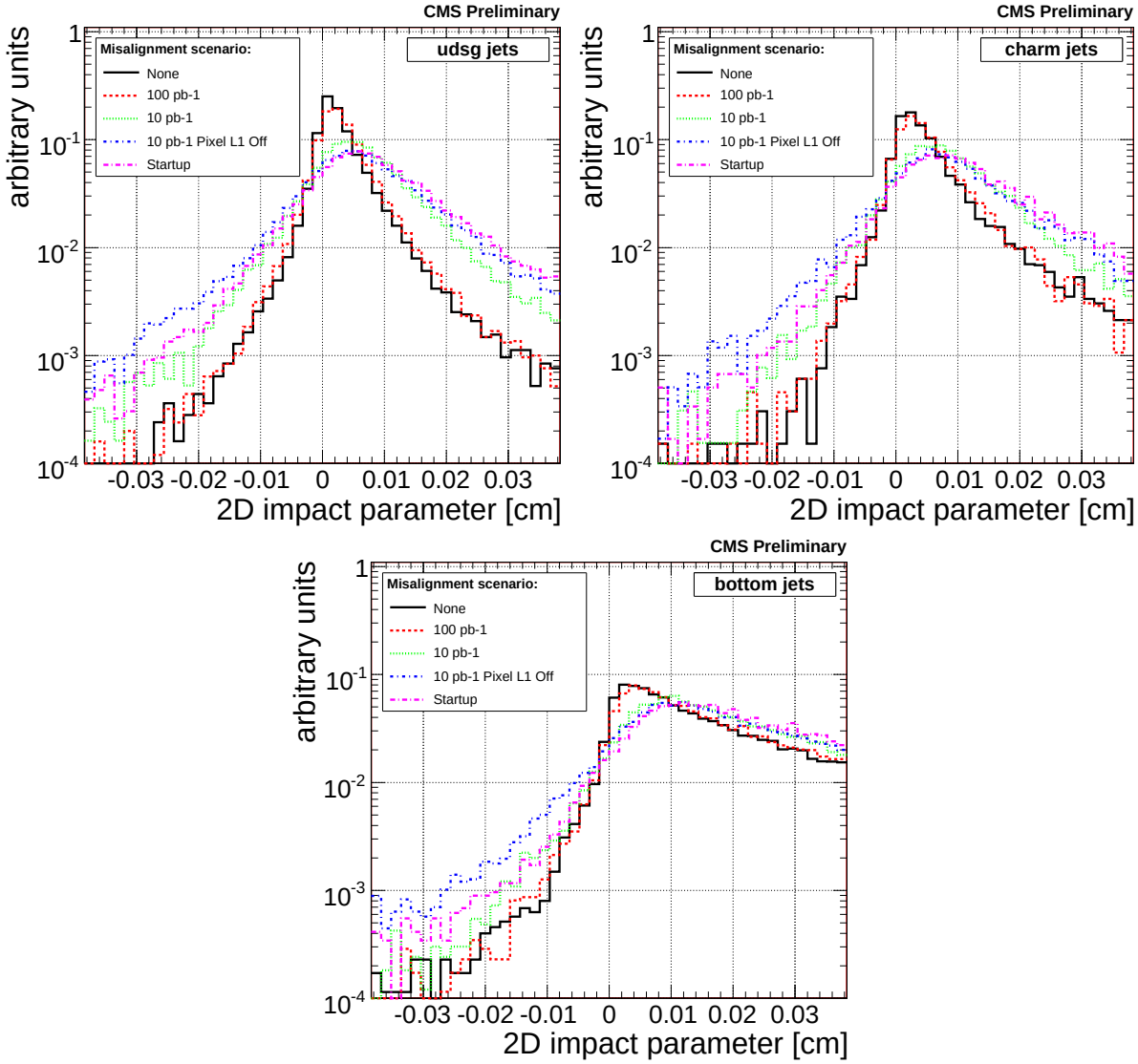

Figure 3: Distribution of the transverse impact parameter measurement *value* of the second track (ordered by I.P. significance) for the various scenarios and jet flavors, presented for light flavor jets (top left), charm jets (top right) and b-jets (bottom).

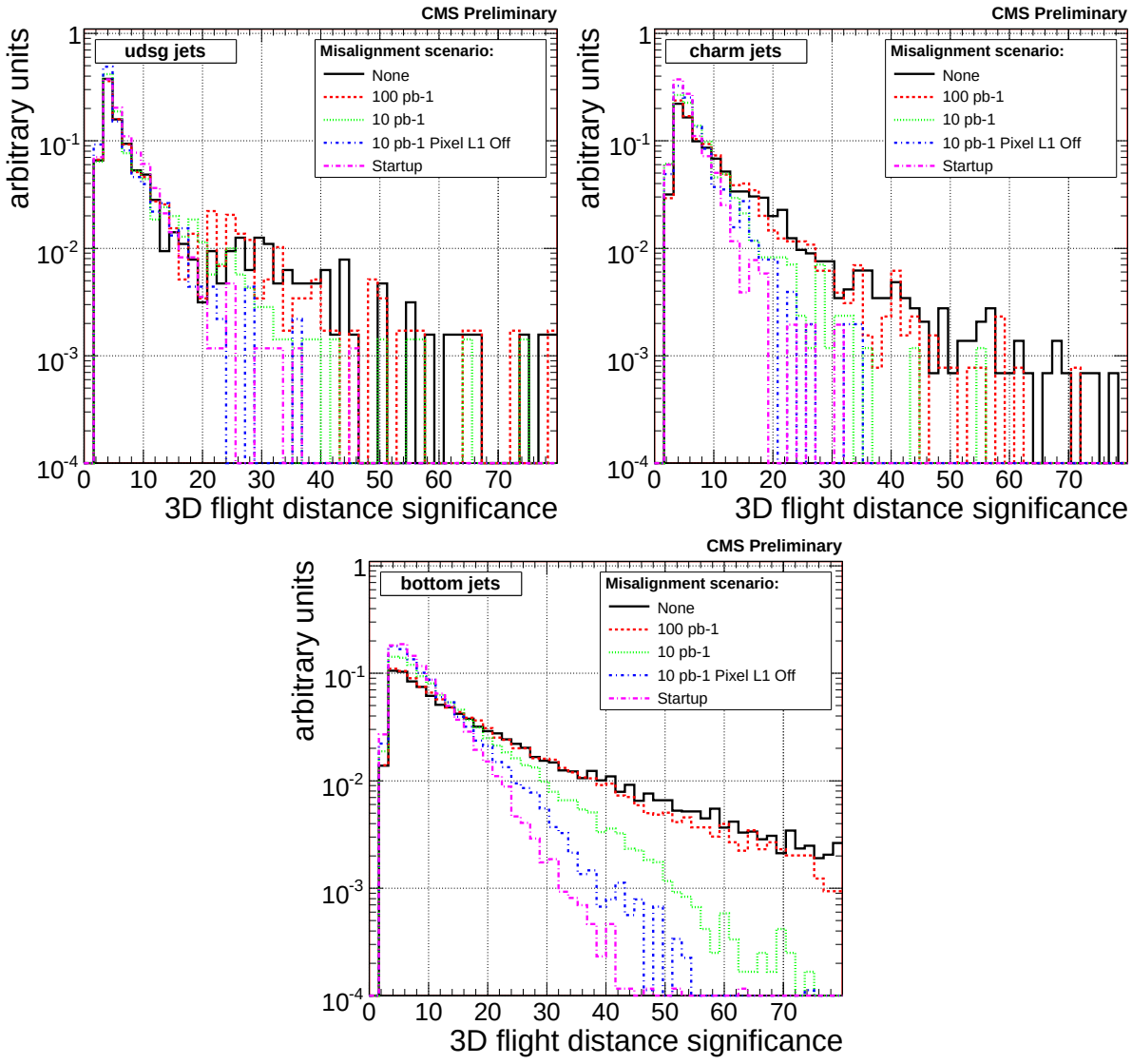

Figure 4: Distribution of the 3D flight distance significance for the various scenarios and jet flavors, presented for light flavor jets (top left), charm jets (top right) and b-jets (bottom).

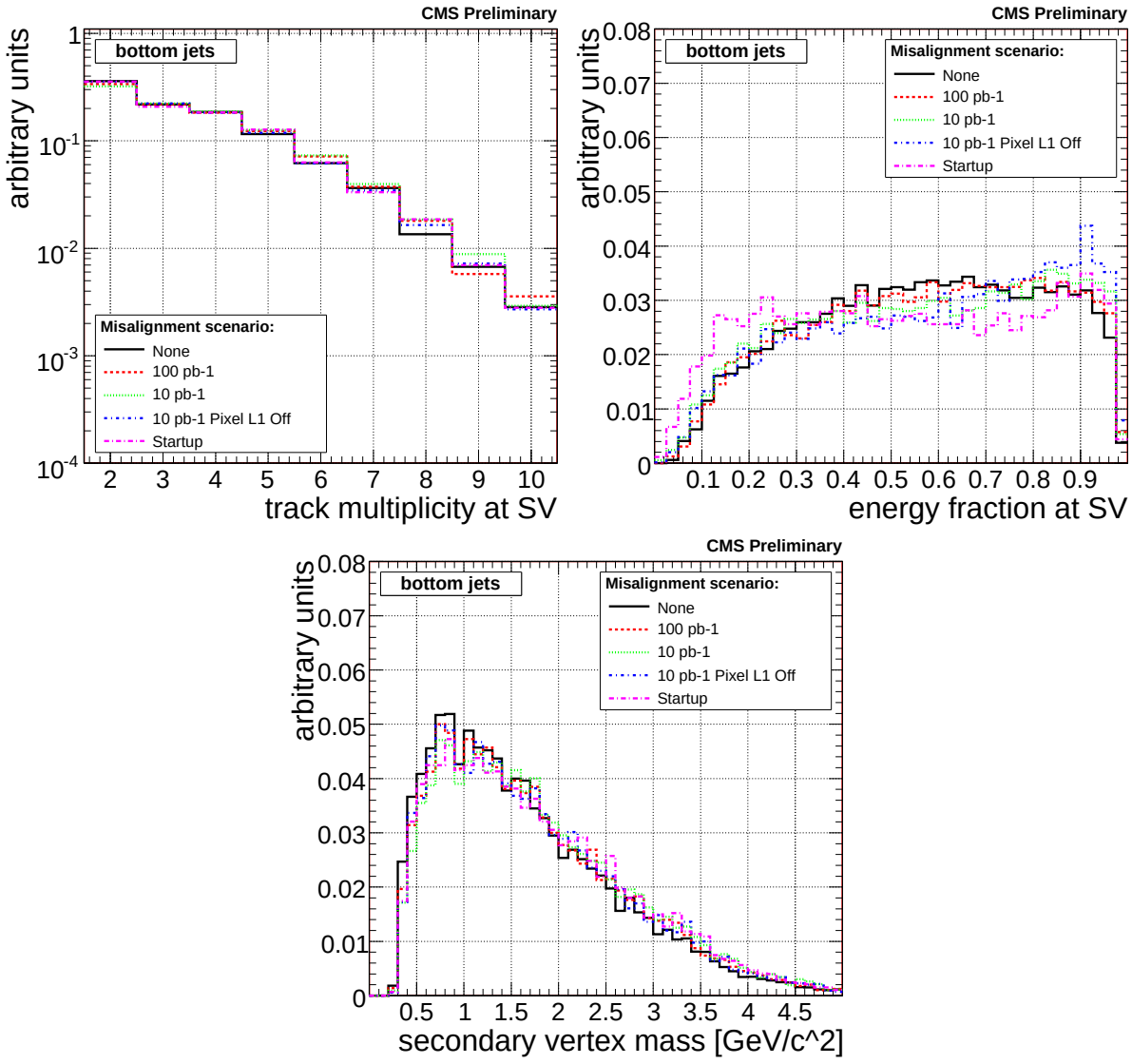

Figure 5: Distributions of track multiplicity (top left), energy fraction (top right) and mass (bottom) of charged tracks at the secondary vertex for b-jets only.

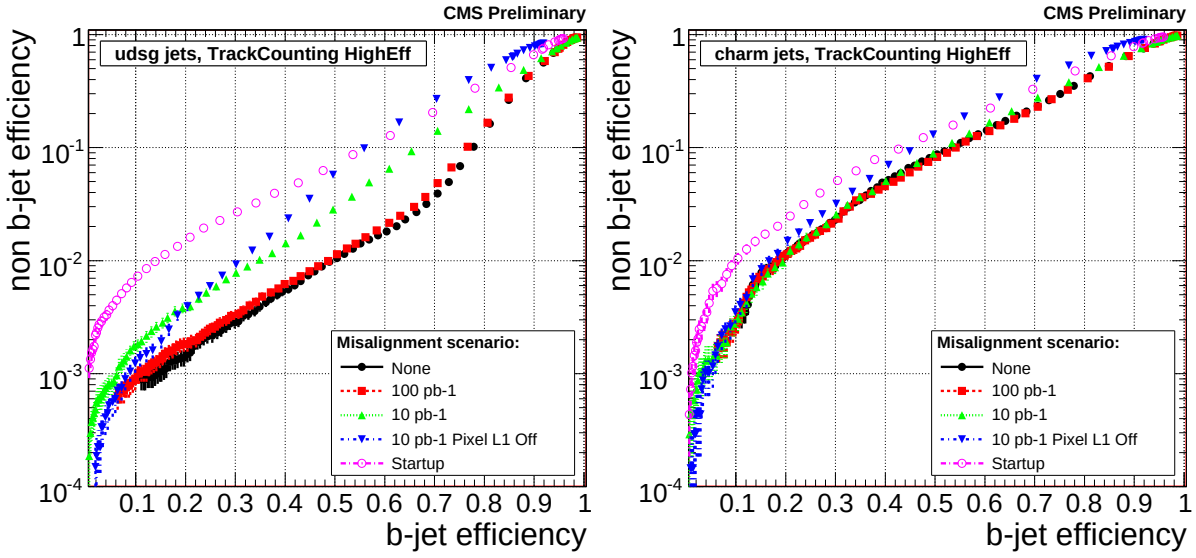

Figure 6: b-jet efficiency versus non b-jet efficiency for the various misalignment scenarios for the TrackCounting (high efficiency) algorithm, presented for light flavor (left) and charm (right) jets.

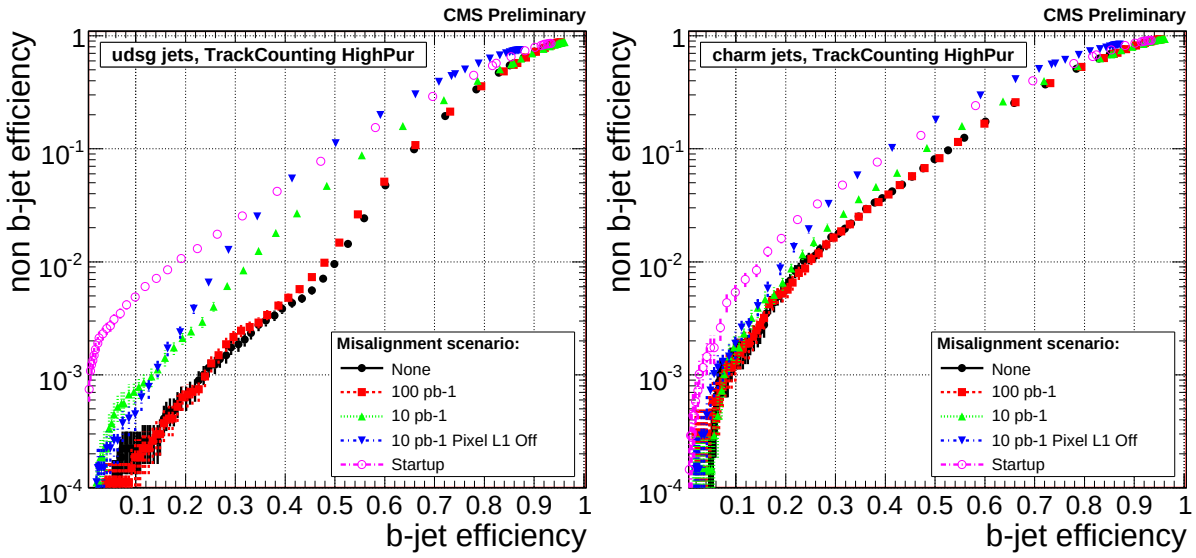

Figure 7: b-jet efficiency versus non b-jet efficiency for the various misalignment scenarios for the TrackCounting (high purity) algorithm, presented for light flavor (left) and charm (right) jets.

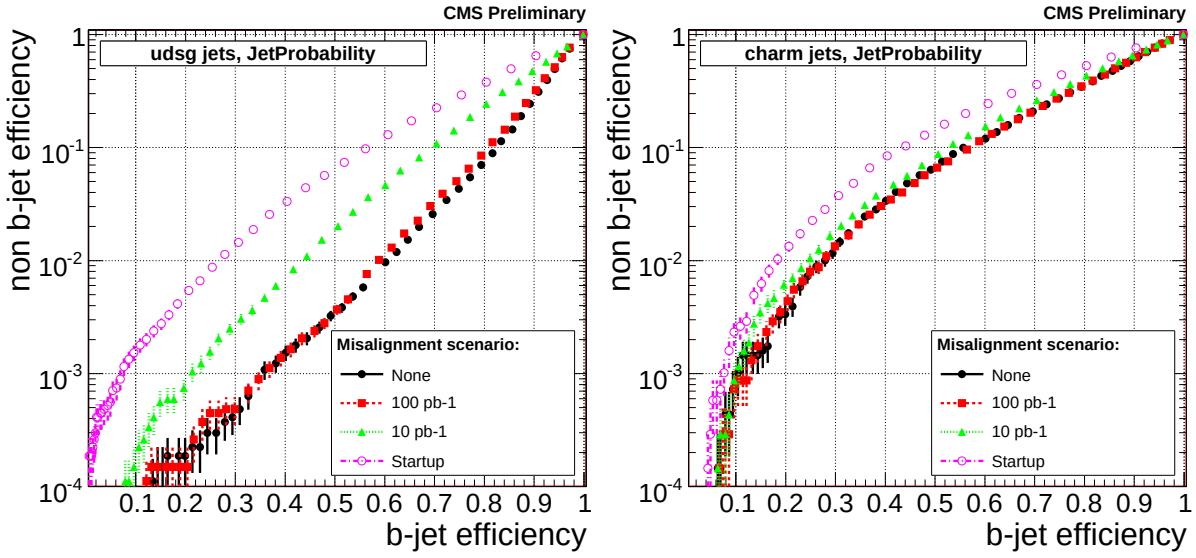

Figure 8: b-jet efficiency versus non b-jet efficiency for the various misalignment scenarios for the JetProbability algorithm, presented for light flavor (left) and charm (right) jets.

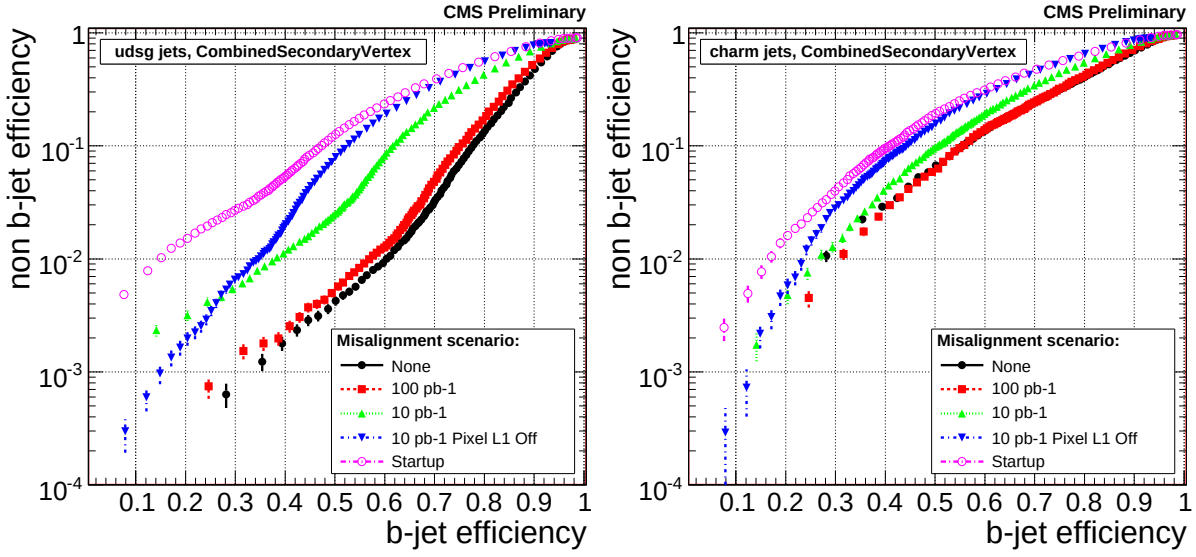

Figure 9: b-jet efficiency versus non b-jet efficiency for the various misalignment scenarios for the Combined Secondary Vertex algorithm, presented for light flavor (left) and charm (right) jets.

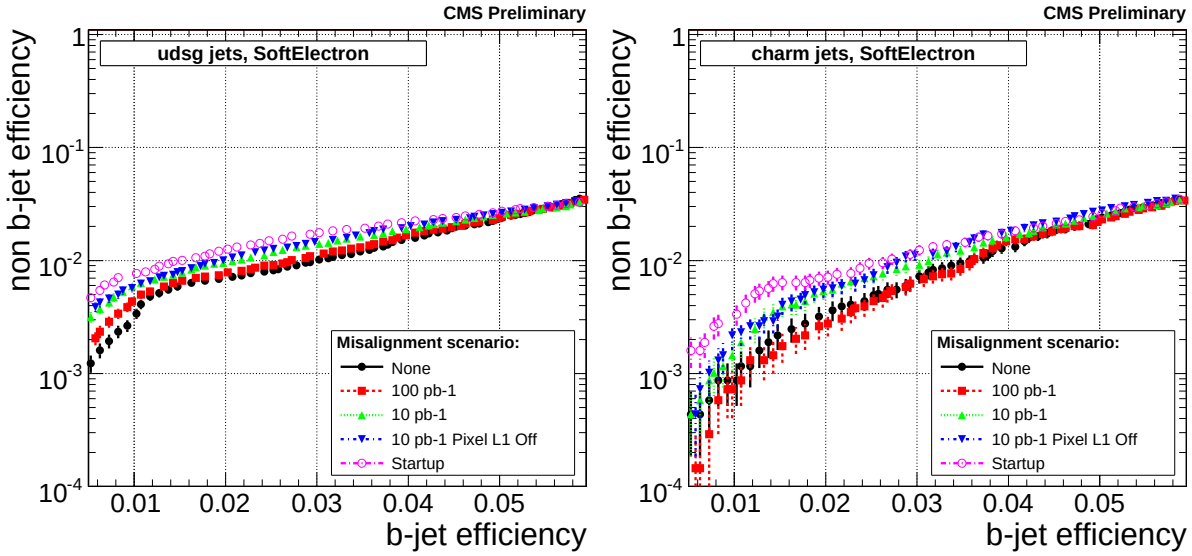

Figure 10: b-jet efficiency versus non b-jet efficiency for the various misalignment scenarios for the SoftElectron algorithm, presented for light flavor (left) and charm (right) jets.

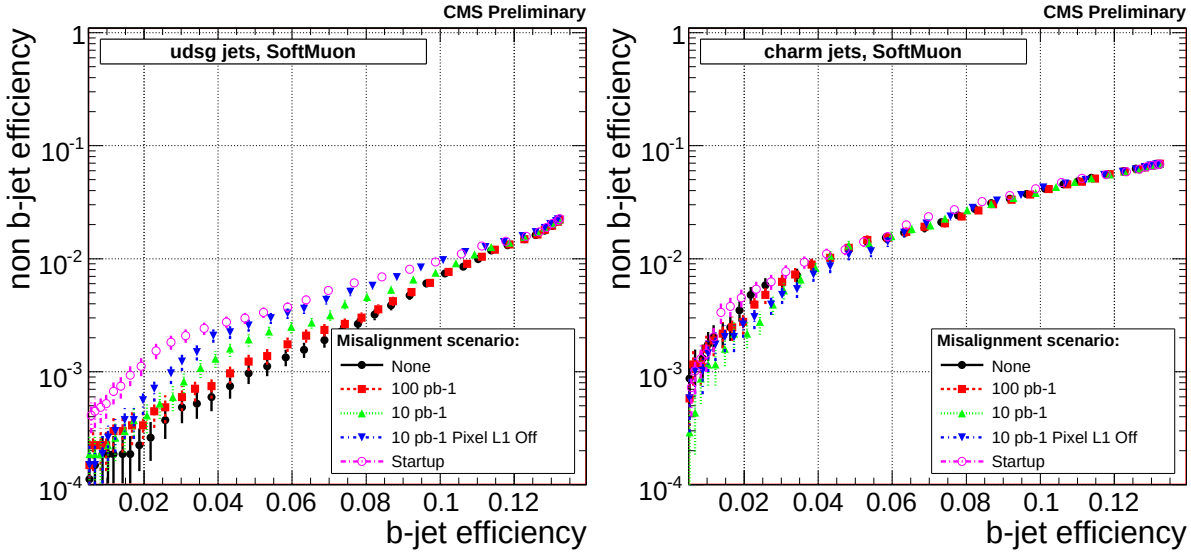

Figure 11: b-jet efficiency versus non b-jet efficiency for the various misalignment scenarios for the SoftMuon algorithm, presented for light flavor (left) and charm (right) jets.

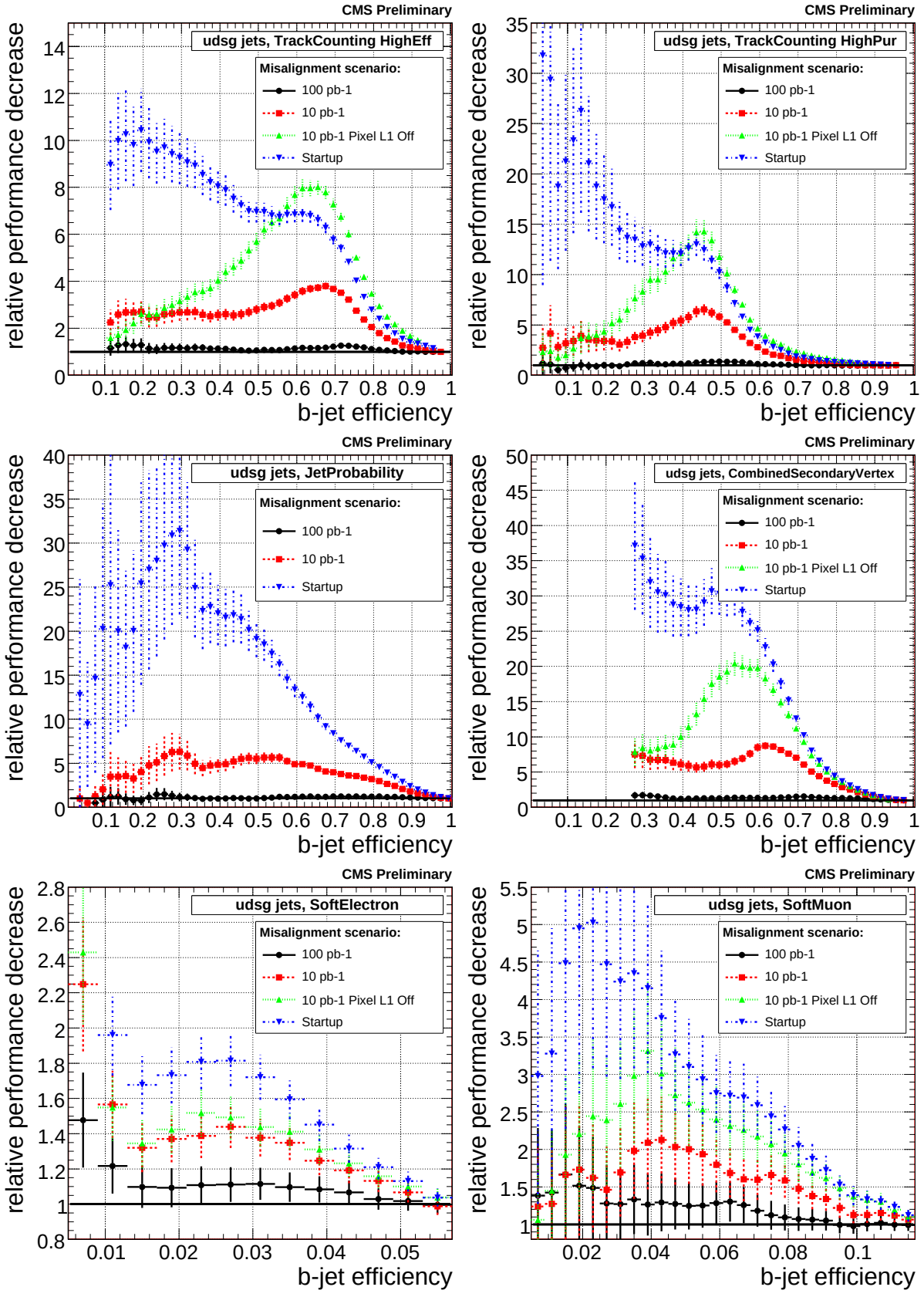

Figure 12: Relative performance decrease ($\epsilon^{mistag}_{misalign}/\epsilon^{mistag}_{align}$) in light flavor mistagging rate versus b-tagging efficiency for the track counting high efficiency (top left) and high purity (top right) algorithms, the jet probability (middle left), the combined SV (middle right), the soft electron (bottom left) and soft muon (bottom right) algorithms.

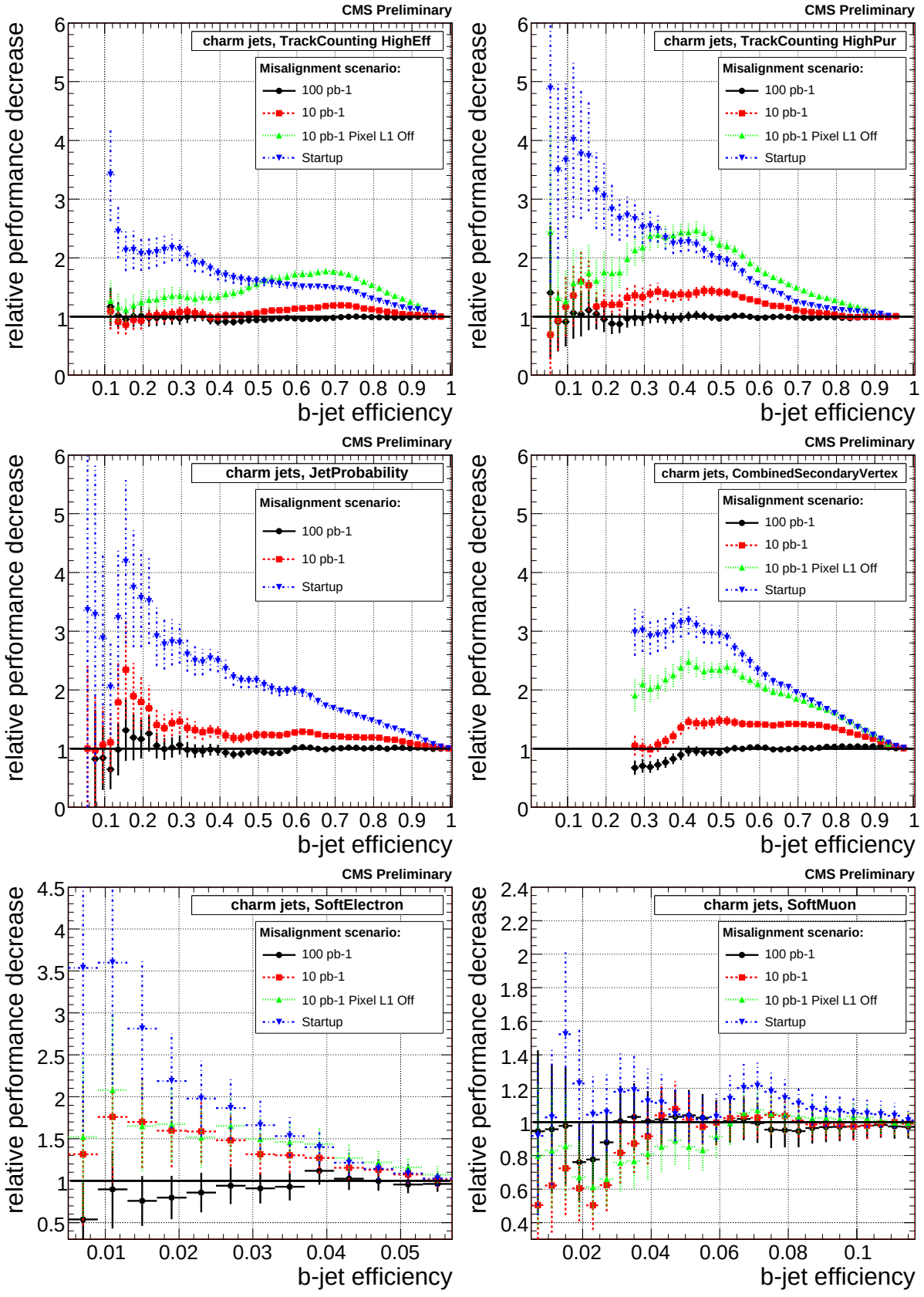

Figure 13: Relative performance decrease ($\epsilon^{mistag}_{misalign}/\epsilon^{mistag}_{align}$) in charm mistagging rate versus b-tagging efficiency for the track counting high efficiency (top left) and high purity (top right) algorithms, the jet probability (middle left), the combined SV (middle right), the soft electron (bottom left) and soft muon (bottom right) algorithms.

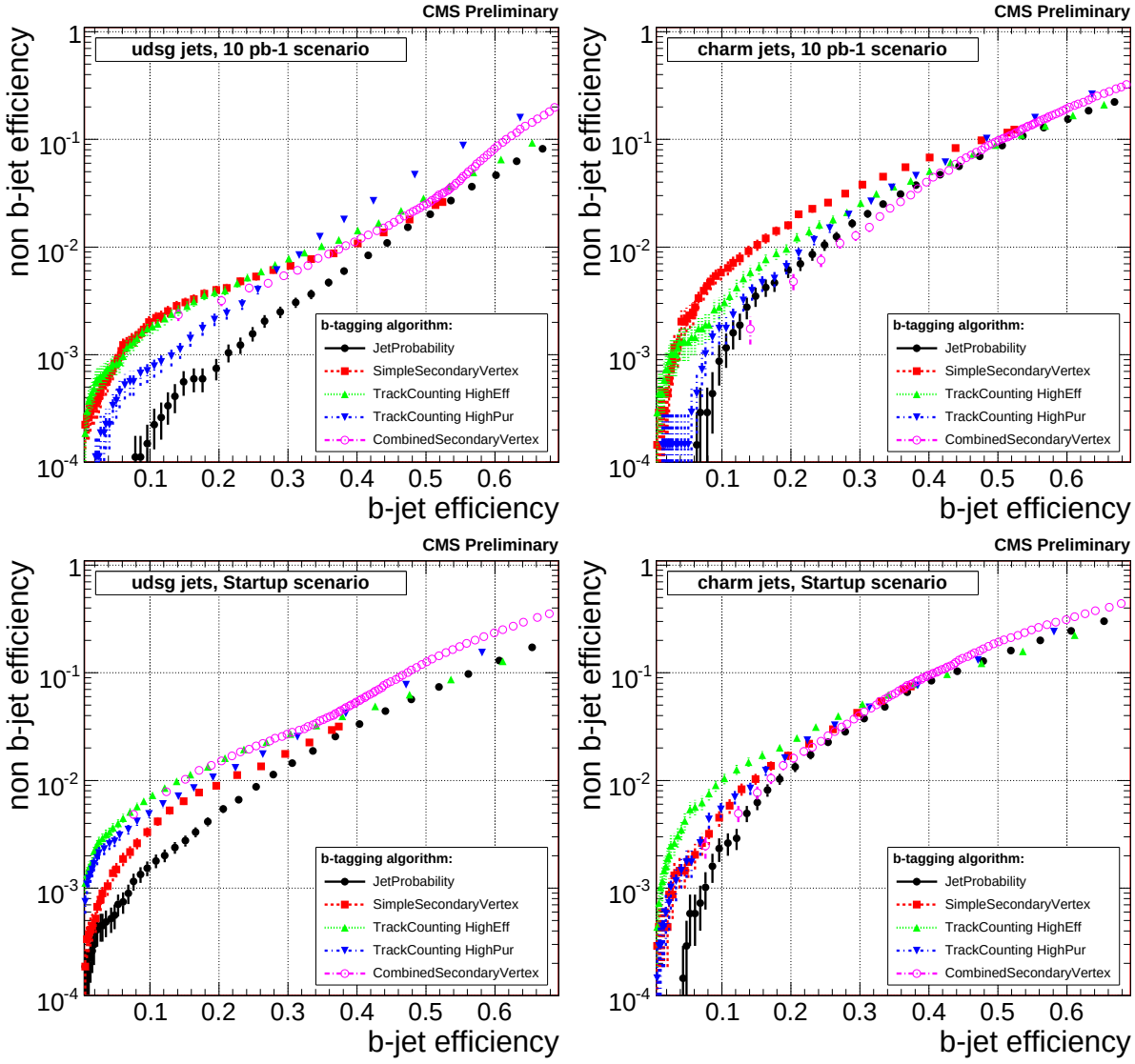

Figure 14: b-jet efficiency versus non b-jet efficiency for the simple secondary vertex tagger in comparison to several other b-tagging algorithms. Distributions are shown for light flavor (left) and charm (right) jets. The upper plots correspond to the 10 pb^{-1} scenario, and the lower ones to the Startup misalignment scenario.

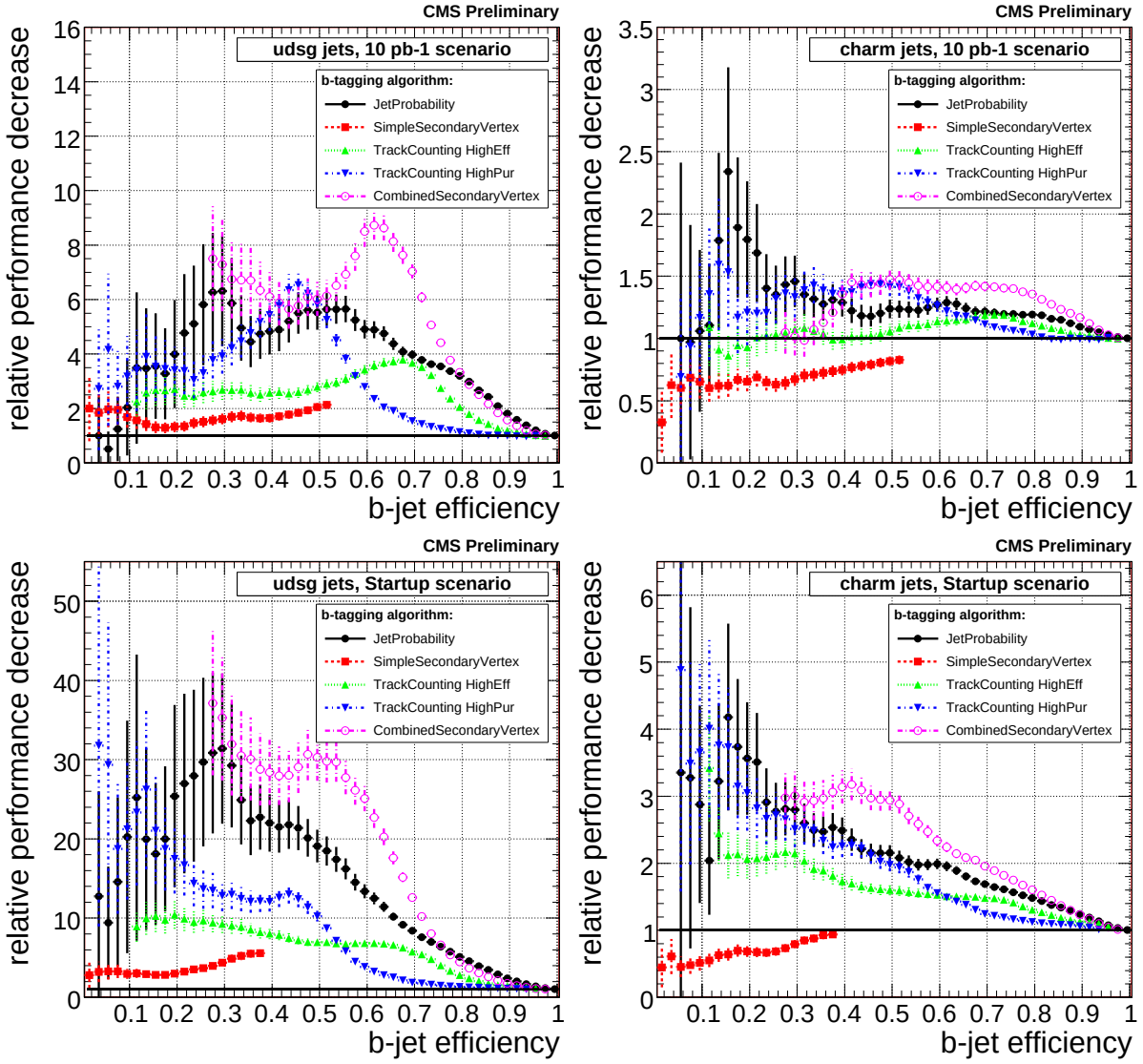

Figure 15: Relative performance decrease ($\epsilon^{mistag}_{misalign}/\epsilon^{mistag}_{align}$) in light flavor (left plots) and charm (right plots) mistagging rate for several taggers compared to a perfectly aligned tracker. The upper plots correspond to the 10 pb^{-1} scenario, and the lower ones to the Startup misalignment scenario.

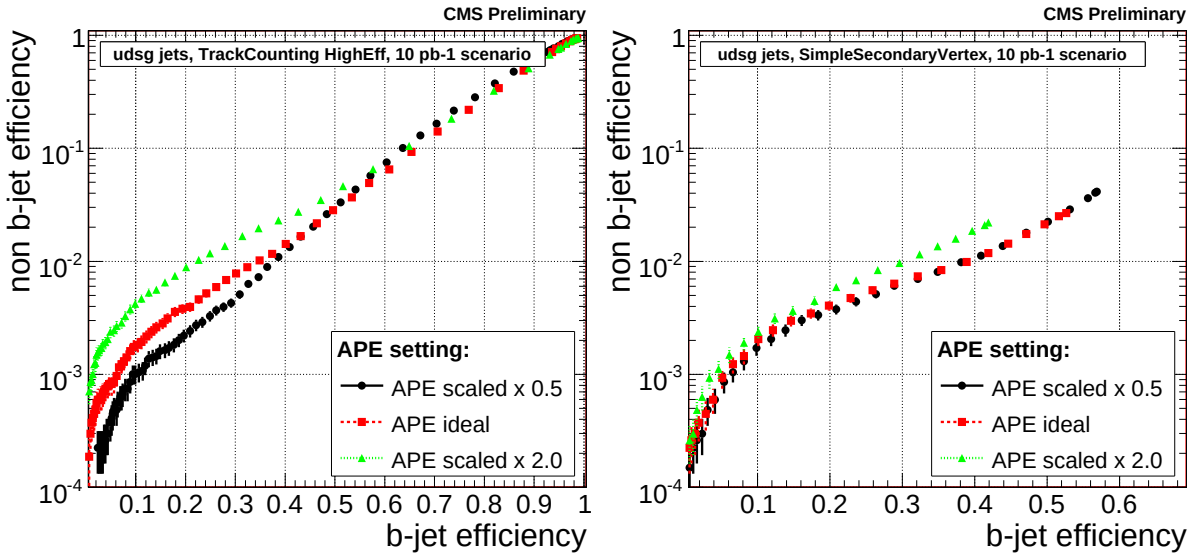

Figure 16: b-jet efficiency versus non b-jet efficiency for the 10 pb^{-1} misalignment scenario shown for the track counting high efficiency (left) and the simple secondary vertex tagger (right) with an alignment position error (APE) that is chosen too large or too small by a factor of two with respect to the ideal value.